Color-Tuning Mechanism in Firefly Luminescence: Theoretical Studies on Fluorescence of Oxyluciferin in Aqueous Solution using Time Dependent Density Functional Theory

Supporting Information.

*Zhong-wei Li [a], Ai-min Ren [a, *], Jing-fu Guo [b], Tianxiao Yang [c] John D. Goddard [c], Ji-kang Feng [a]*

a. State Key Laboratory of Theoretical and Computational Chemistry, Institute of Theoretical Chemistry, Jilin University, Changchun 130023, P. R. China

b. College of Physics, Northeast Normal University, 130024, P. R. China

c. Department of Chemistry, University of Guelph, Guelph, Ontario, Canada N1G 2W1

* Corresponding author: Fax: 0431-88945942; E-mail address:aimin.ren@gmail.com

Full reference for Gaussian03. (31) Frisch, M.J.; Trucks, G.W.; Schlegel, H.B.; Scuseria, G.E.; Robb, M.A.; Cheeseman, J.R.; Montgomery Jr., J.A.; Vreven, T.; Kudin, K.N.; Burant, J.C.; Millam, J.M.; Iyengar, S.S.; Tomasi, J.; Barone,V.; Mennucci, B.; Cossi, M.; Scalmani, G.; Rega, N.; Petersson, G.A.; Nakatsuji, H.; Hada, M.; Ehara,M.; Toyota, K.; Fukuda, R.; Hasegawa, J.; Ishida,M.; Nakajima, T.; Honda, Y.; Kitao, O.; Nakai, H.; Klene, M.; Li, X.; Knox, J.E.; Hratchian, H.P.; Cross, J.B.; Adamo, C.; Jaramillo, J.; Gomperts, R.; Stratmann, R.E.; Yazyev, O.; Austin, A.J.; Cammi, R.; Pomelli, C.; Ochterski, J.W.; Ayala, P.Y.; Morokuma, K.; Voth, G.A.; Salvador, P.; Dannenberg, J.J.; Zakrzewski, V.G.; Dapprich, S.; Daniels, A.D.; Strain, M.C.; Farkas, O.; Malick, D.K.; Rabuck,A.D.; Raghavachari, K.; Foresman, J.B.; Ortiz, J.V.; Cui, Q.; Baboul, A.G.; Clifford, S.; Cioslowski, J.; Stefanov, B.B.; Liu, G.; Liashenko, A.; Piskorz, P.; Komaromi, I.; Martin, R.L.; Fox, D.J.; Keith, T.; Al-Laham, M.A.; Peng, C.Y.; Nanayakkara, A.; Challacombe, M.; Gill, P.M.W.; Johnson, B.; Chen, W.; Wong, M.W.; Gonzalez, C.; Pople, J.A. *GAUSSIAN-03*, *Revision A.1*, **2003**, *Gaussian*, *Inc., Pittsburgh*,*PA*.

.

1. Bond lengths of the molecules referred to in the text.

Figure S1. Optimized geometries in S_1 of the enol0, keto0, enol-1, keto-1, enol-2, keto+1 and twist-keto-1 forms by TD B3LYP/6-31+G*; All optimizations were carried out in the gas phase. The bond lengths are in Angstrom. C-H bond lengths are not shown.

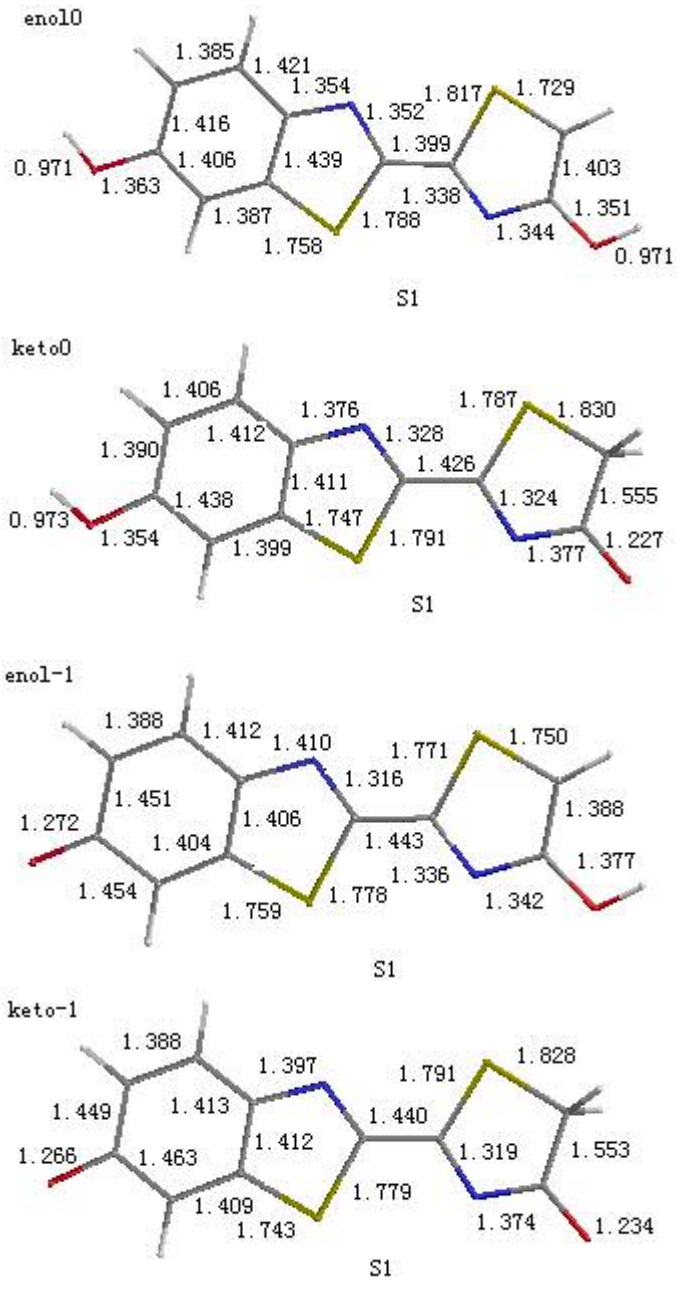

enol-2

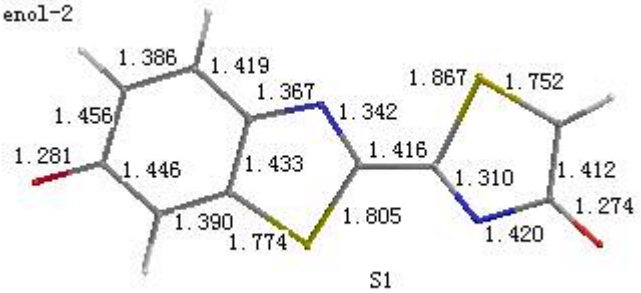

S1

keto+1

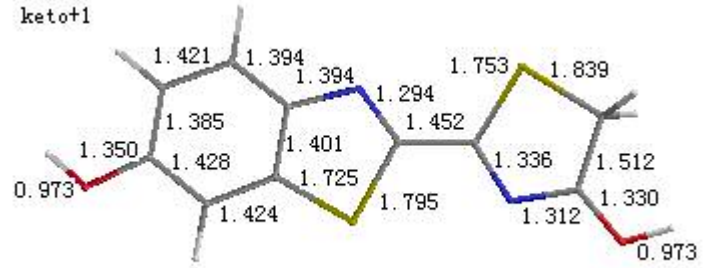

S1

twist-keto-1

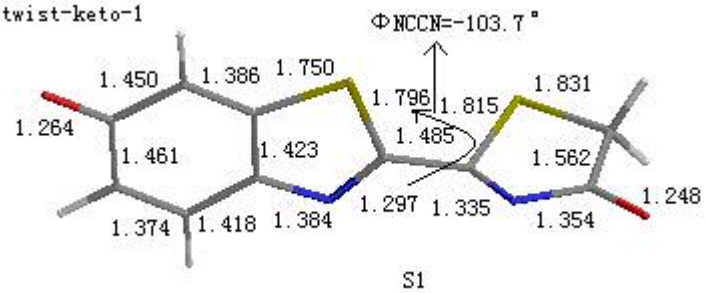

S1

Figure S2. Optimized geometries of S_1 of [enol-2]-2Na complex by CIS/6-31G* and CIS/6-31G* with the PCM for water; the bond lengths are in Angstrom. C-H bond lengths are not shown.

Comparing the geometry of the sodium complex in the gas phase with that including the PCM for water, larger differences occur. It is necessary to consider solvent effects on the excited state geometry.

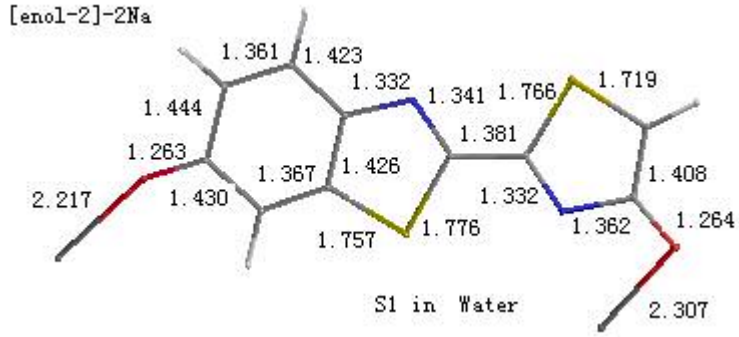

2. The differences in geometries due to different B3LYP functionals in Turbomole and Gaussian03.

Figure S3. Optimized geometries in S_0 of keto-1 by B3LYP/6-31+G* in Turbomole and Gaussian03; the bond lengths are in Angstrom. C-H bond lengths are not shown.

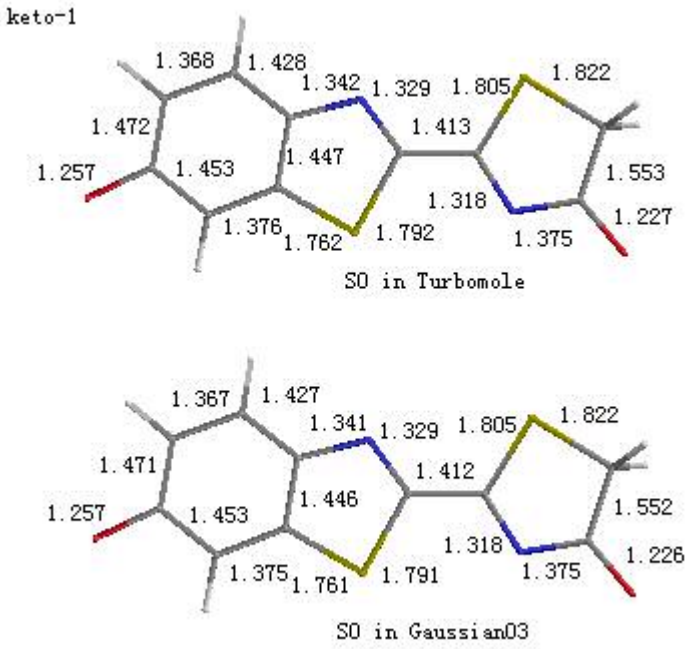

There are no significant differences between the two geometries due to the different implementations of B3 in the two programs. In addition, based on the excited state geometry of keto-1, the excitation

energies calculated by TD B3LYP/6-31+G* with Turbomole and Gaussian03 respectively are 556.20 nm and 555.80 nm. Thus there are essentially no differences between Turbomole and Gaussian03 for predictions on oxyluciferin molecules due to the different implementations of the B3 functional.

3. Charge transfer in planar and twisted structures.

Figure S4. Charge Distribution, in a.u., of the keto-1, and the twist-keto-1 forms predicted by B3LYP/6-31+G* (S_0) and CIS/6-31+G* (S_1) methods in the gas phase based on TD B3LYP/6-31+G* optimized geometries.

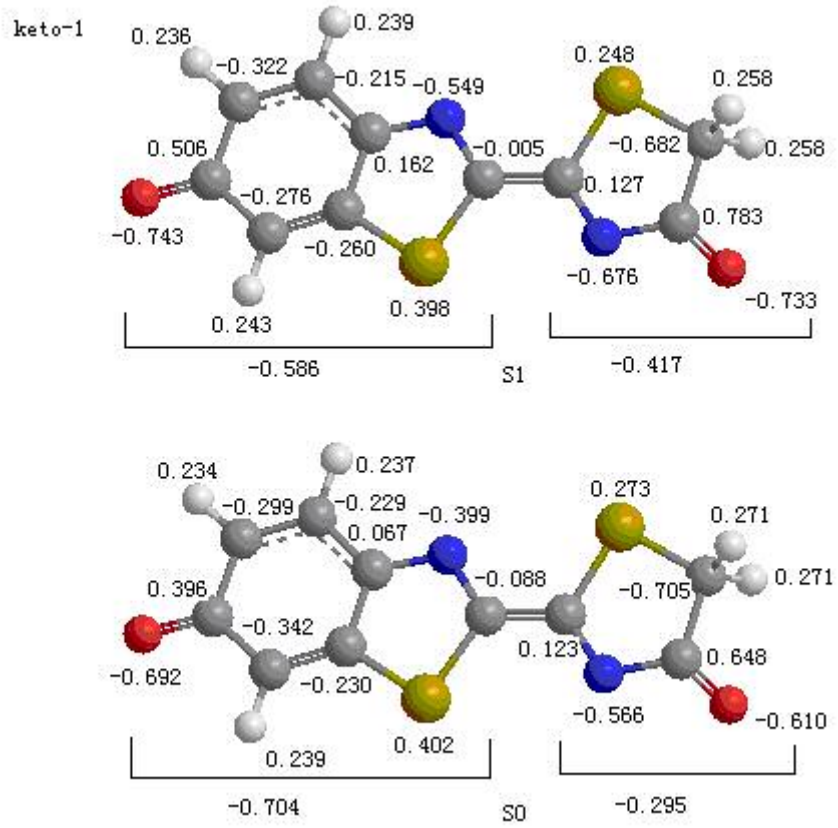

twist-keto-1

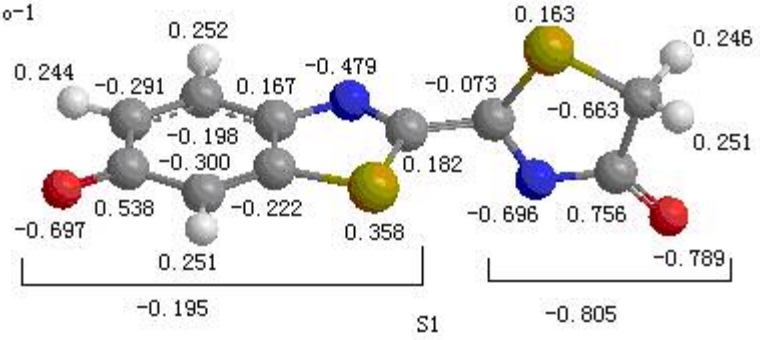

S1

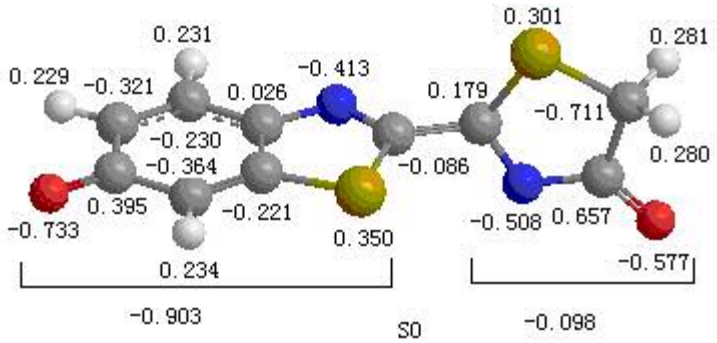

S0

4. Charge transfer in the Na-complex in the gas phase.

Figure S5. Charge Distribution, in a.u., of [enol-2]-2Na predicted by the B3LYP/6-31+G* (S_0) and CIS/6-31+G* (S_1) methods in the gas phase based on CIS/6-31G* optimized geometries. The total charges predicted for the benzothiazole and thiazoline moieties of [enol-2]-2Na do not include the charges on the sodiums.

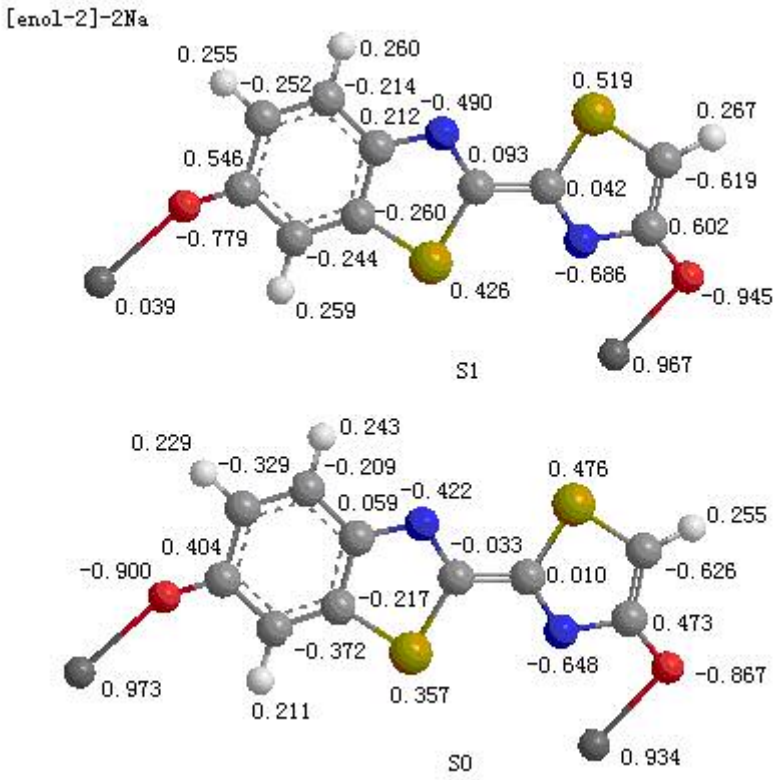

5. Charge distributions of enol-2 and its Na-complex in water in the excited state.

Figure S6. Charge Distribution, in a.u., of the enol-2 and the [enol-2]-2Na complex predicted by the CIS/6-31+G* methods in the water phase based on CIS/6-31G* with PCM optimized geometries. The total charges predicted on the benzothiazole and thiazoline moieties of [enol-2]-2Na do not include the charges on the sodium.